Ion-Sensitive Tunnel Field-Effect Transistor Based Wearable Sweat Sensor for High-Sensitivity and Wide Dynamic Range pH Sensing

Muhammad Johirul Islam[1] and Md. Iqbal Bahar Chowdhury[1*]

[1]Department of Electrical and Electronic Engineering, United International University, Dhaka, Bangladesh.
iqbal@eee.uiu.ac.bd

Abstract. Demands of ultra-scaled ion sensitive field effect transistors (ISFETs) with higher current sensitivity and wider dynamic pH range are sky-rocketing as the ISFET devices find their increasing applications in the arena of wearable sweat sensors. In this context, a scaled tunnel FET (TFET) can serve as a very attractive and highly promising FET architecture that can be associated with an ISFET device for superior performance metrics. In this work, a p-i-n tunnel FET (TFET)-based simple ISFET has been implemented and investigated in Cadence simulation framework. Simulation results reveal that the subthermionic subthreshold swing of the TFET can enhance the current sensitivity beyond the maximum theoretical limit, whereas, the ambipolarity of the TFET along with appropriate gate tuning can widen the dynamic range. Therefore, the proposed TFET-based ISFET sensor has excellent promise in the realization of high-density chips with improved performance increasingly demanded by the wearable sweat sensors and hence, can meet the requirements of the sustainable development goal (SDG) 3.

Keywords: ISFET, TFET, pH Sensor, Sensitivity, Dynamic Range, SDG 3.

R. Rzayev et al. (eds.), *Proceedings of the International Conference on Current Problems in Engineering and Applied Sciences (ICCPEAS 2025)*, Advances in Engineering Research 299,
https://doi.org/10.2991/978-94-6239-668-5_41

1 Introduction

Recently, ISFETs offer a very attractive platform for wearable sweat sensors [1, 2] as compared with the solid-state ion-selective electrodes because of their capability of ultra-miniaturization, low power consumption, high sensitivity, CMOS-compatible integration, less output-signal degradation and less noise [2]. Sweat contains several biomarkers such as ions (i.e., Na+, K+), weak acids/bases, lactate, glucose, hormones, and heavy metals (i.e., Cd2+, Pd2+), etc. [3]. Therefore, ISFETs for sweat sensors need to be extremely scalable for the feature-compatibility with these biomarkers. However, the device scaling requires aggressive downscaling of the associated FET device with increased doping levels and reduced oxide thickness [4], following the scaling rules. Such aggressive downscaling results in various short-channel effects (SCEs) [5], and non-idealities [6]. Specifically, SCEs lead to the non-scalability in the threshold voltage, and hence, in the subthreshold swing (SS) [5]. Since the current sensitivity (S_I), defined as the logarithmic change in the drain current per unit change in pH [2], is inversely related with the SS [5], downscaling of ISFET severely degrades its value from its theoretical maximum of 1 dec/pH [5]. On the other hand, dynamic range is defined as the range of analyte concentration that a sensor can readily and reliably detect and quantify [8] and hence, a wider dynamic range is a must requirement for wearable sweat sensors where the concentrations of the biomarkers vary widely [3]. Sensors with narrow dynamic range have restricted applications where the concentration levels of the target analyte vary within a narrow range [8]. The choice of appropriate channel and oxide materials of the associated FET devices can significantly impact the 'power-sensitivity' issues of the ISFET devices. In the literature, various high-mobility materials (GaAs [7], carbon nanotube [9], InAs [10-11], graphene [12], SiGe [13] etc.) and high-κ dielectrics (Al_2O_3 [10], HfO_2 [11] etc.) are investigated as channel and oxide materials, respectively. Employing steep-slope, CMOS-compatible FET devices like negative capacitance FETs (NCFETs) and tunnel FETs (TFETs) can enhance the current sensitivity to reach beyond the limit of 1 dec/pH. An NCFET-based ISFET sensor with current sensitivity > 1 dec/pH has been proposed by Bellando et al. [14]. However, NCFET-based ISFETs require additional fabrication steps to introduce a ferroelectric material as well as to ensure the stable operation of the negative capacitance, making them a costlier option.

Tunnel FETs are emerged as the attractive alternative of scaled down MOSFETs for ultra-low-power driven switching applications with sub-0.5 V logic operations [15]. These FETs exhibit almost the same drain current for both positive and negative gate voltages in their transfer characteristics- a distinctive property called as the ambipolarity property [8]. Utilizing this ambipolarity property, Ajay et al. [16] sensed the positively charged bio-molecules by the 'normal' conduction and the negatively charged bio-molecules by the 'ambipolar' conduction. Lee et al. [17] utilized this ambipolarity for multi-sensing of positively/negatively charged bio-molecules with almost equivalent sensitivity. Kalra et al. [8] exploited this ambipolarity to dynamically widen the dynamic range by tuning the gate bias appropriately. Consequently, appropriate utilization of 'ambipolarity' of TFETs can be promising for extending the measurable pH-range (dynamic range) in ISFET-based pH sensors. However, to ensure the ambipolarity effectively, simple p-i-n tunnel FET needs to be employed, as ambipolarity is more dominant in the p-i-n TFETs than in p-n-p-n TFETs (conventionally used in biosensing applications [18]). This work, therefore, aims to investigate the feasibility of TFET architecture based ISFET sensor to achieve a current sensitivity > 1 dec/pH and a widened dynamic range. Simulation results in Cadence environment show that the TFET based ISFET sensor has a higher SI (> 1 dec/pH) and a wider dynamic range (pH range: 5.0-12.0) than their MOS-based counterparts. Therefore, the proposed ISFET has promises of the realization of high-density sweat sensor chips, thereby ensuring the good health and well-being of the mass people i.e. meeting the sustainable development goal 3 (SDG 3).

2 Simulation Methodology

Device Structure

The response of an ISFET to pH varies with the geometry and material of the FET device and depends on the biasing condition. Commonly ISFETs are operated in the unsaturated region. Recently, operation of ISFETs under weak inversion condition becomes of interest due to the ability of the lower power consumption [5,19] and the achievement of the higher sensitivity [20]. It is noteworthy to mention that the power consumption of a TFET under subthreshold operation is less than its MOS counterpart [15]. Therefore, all the sensors used in this work are biased in the subthreshold region. The 3D schematic of a simple p-i-n TFET-based ISFET pH sensor is presented in Fig. 1 (a), where an aqueous solution is used as the electrolyte, silicon is the channel material and SiO_2 is used as the oxide material.

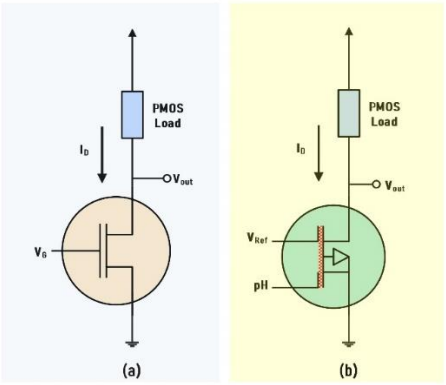

Fig. 1. (a) A TFET-based common-source amplifier circuit. (b) Proposed common-source like TFET based ISFET sensor.

Very similar to a common-source TFET amplifier shown in Fig. 1 (b), the proposed TFET-based ISFET pH sensor has been implemented, where an ISFET sensor acts as the driver device and a p-MOSFET is used as the load device. The sensors are based on two different FET structures- a conventional MOSFET and a single gate p-i-n hetero-junction tunnel FET. In the proposed configuration, for a constant gate reference voltage (V_{Ref}), the pH level modulates the effective gate voltage ($V_{g,eff}$) of the ISFET for which the drain current varies.

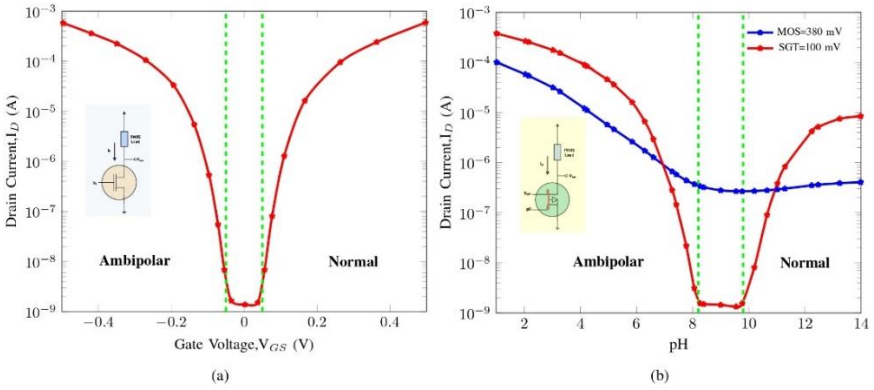

Fig. 2. (a) Simulated transfer characteristic curve of a p-i-n single-gate tunnel (SGT) FET. (b) The drain current vs. pH curves for the SGTFET- and MOSFET-based ISFET sensors biased with a reference gate voltage V_{Ref} of 100 mV and 380 mV respectively.

Simulation Approach

Since hardware-level implementation of devices and projects incurs cost of materials and fabrication as well as stress and processing time, simulation approach is preferable for thorough investigation and analysis. Widely used simulation tools include

MATLAB, TCAD, Proteus, Simulink and Cadence. MATLAB is appropriate for analytical modeling of devices such as BJT [21], HBT [22], solar cell [23-24] etc. TCAD is used for device level design and modeling for advanced FETs [25-27], wherein numerical techniques can resolve the analytical intractability of device modeling. Proteus can be used to simulate and analyze circuit-level performance [28-29], whereas, Simulink can be used to model and analyze large systems [30-31] On the other hand, Cadence has the ability of both device and circuit level modeling and characterization using Verilog-A models [5], SPICE models [9] and built-in TSMC models [32-34]. Therefore, the ISFET sensor investigated in this work has been simulated in the Cadence environment. To simulate the behavior of the ISFET in HSPICE, verilog etc., the behavioral macromodel developed by Martinoia *et al.* [35] has been employed. Using this model an ISFET can be decoupled into two stages: an electronic stage composed of any FET device and an electrochemical stage representing the electrolyte-oxide interface. Dak *et al.* [36] modelled the ISFET sensor as a combination of a pH-dependent nonlinear voltage source, V_{pH} and a FET device, where V_{pH} captures the pH-dependency of the sensor and the FET is driven by the effective gate voltage ($V_{g,eff}$) given by

$$V_{g,eff} = V_{pH} + V_{Ref} \quad (1)$$

where V_{Ref} is the biasing voltage applied to the reference electrode. In order to implement the ISFET-based sensors in Cadence Virtuoso Environment, experimentally verified verilog-A models have been employed for the electrochemical stage [5], for the conventional MOSFET device and for the tunnel FET, which is an AlGaSb/InAs-based single-gate p-i-n heterojunction structure [37].

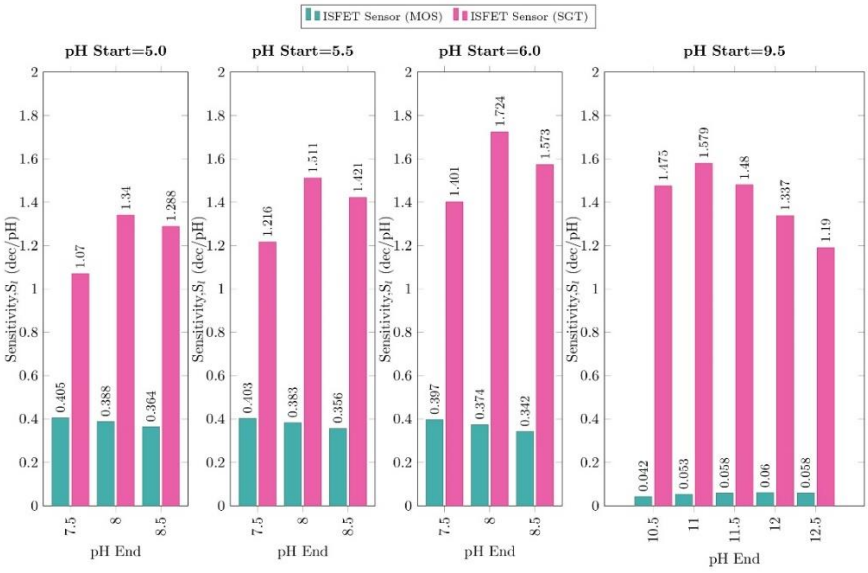

Fig. 3. The current sensitivity variation against the measurable pH ranges for (a) 'normal' and (b) 'ambipolar' conduction of SGT- and MOS-based sensors.

3 Results and Discussion

This section presents the results of the simulations carried out in Cadence as well as analyses and discusses whether the tunnel FET (TFET) structure enhances the sensitivity of the ISFET or not.

Figure 2(a) shows the simulated transfer characteristic curve of a p-i-n single-gate tunnel FET, which is very similar to the experimentally characteristics curves obtained in the literature [18]. This plot also shows the unique ambipolar' conduction which is almost identical with the 'normal' conduction for a p-i-n tunnel FET [18]. Figure 2(a) plots the transduction of the pH level of the electrolyte solution to the drain current of an SGT- and a MOS-based ISFET sensors biased with a constant reference gate voltage (V_{Ref}). The trend of the observed I_D vs. pH curved can be explained as follows. From the electrochemical point of view, for an aqueous solution, the oxide surface of the ISFET devices is electrically neutral at pH = 7.0, known as the isoelectric point, pI [38] and getting more positively (negatively) charged as the pH level decreases (increases) from the pI [38]. In other words, it can be argued that as the pH level increases from pH = 1.0, the electrochemical potential V_{pH} (which is caused by the change in the pH level) starts to decrease, eventually reaches to zero at pH = pI and becomes increasingly negative for pH > pI. Hence, the changes in the pH level with V_{Ref} = constant, modulates the effective gate voltage ($V_{g,eff} = V_{Ref} + V_{pH}$) resulting in different gate biasing conditions for an ISFET. For small and positive V_{Ref}, the device works in the linear/subthreshold condition in 'normal' conduction at pH = 1.0 and moves to the 'Off' condition as pH increases [Fig. 2 (b)]. The device is in the 'Off' state for a pH range of 8.0-9.0 (pH >lpI). However, for even larger values of pH (> 9.0), the response of the ISFET devices depends on the FET architecture: for MOS-based ISFET, the device remains in the 'Off' state i.e $I_D \rightarrow 0$, whereas, for SGT-based ISFET, the device enters in the 'ambipolar' conduction due to the tunnel FET's unique 'ambipolar' characteristics [18] and hence, the device follows the trend of the 'normal' conduction. In other words, because of the ambipolar behavior of the p-i-n TFETs, SGT-based sensors have two distinct measurable pH ranges and hence the dynamic range becomes widened: one covers the pH ≈ 5.5−8.0 and the other spans in pH ≈ 10.0−12.5; for MOS-based sensors this range covers only pH ≈ 5.5−9.0 [Fig. 2(b)]. Another observation of Fig. 2 (b) suggests that the SGT-based sensor may have higher current sensitivity than its MOS-based counterpart because of the observed sharper change in the drain current for a given pH change. The bar plots of Fig. 3 show the effects of varying the measurable pH ranges on the sensitivity for both SGT and MOS-based ISFET sensors, where the measurable pH range can be varied by changing the bounding limits, pH_{Start} and pH_{End}. Several observations can be made from these figures. First, the SGT-based sensor has more than two times higher sensitivity than its MOS-based counterpart in 'normal' conduction, which can be attributed to the TFET's lower subthreshold swing; indeed, the SGT-based sensor shows a current sensitivity > 1 dec/pH (the theoretical maximum value) for all the measurable ranges, whereas, the MOS-based sensor has a much lower current sensitivity (S_I < 0.403 dec/pH). Moreover, the sensitivity of MOS-based sensor becomes trivial as compared with the SGT-based sensor in 'ambipolar' conduction, as MOSFETs have no such conduction. Therefore, it can be concluded that SGT-based sensors maintain a

current sensitivity greater than the theoretical maximum for a wider dynamic range in pH, which spans from the 'normal' conduction to the 'ambipolar' conduction except for a brief 'Off' region.

Fig. 4 (a) shows the effect of increased gate bias on the drain current of both MOS and SGT-based ISFET sensors when operating in the 'Off' mode (pH ranges from 7.5-9.5). In both these sensors, the increased gate bias results in higher drain currents, as both devices are moved to operate in the subthreshold region instead of the 'Off' region. For the same amount of bias increase, the MOS-based sensor experiences a steady and almost one of order current increase, whereas, a sharper and several order of higher current is observed in the SGT-based ISFET sensor [Fig. 4 (a)]. Particularly, by applying appropriate gate bias for the SGT-based ISFETs, an increased and almost the same sensitivity can be ensured for all three regions ('normal', 'Off' and 'ambipolar' regions) and hence, the measurable pH range i.e. the dynamic range can be widened.

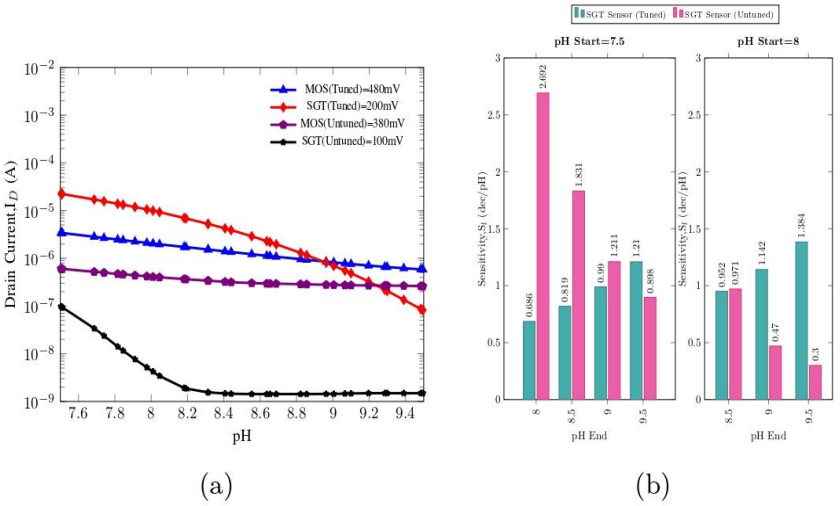

Fig. 4. (a) Effect of the gate tuning on the drain current in the 'Off' mode for both the MOS- and TFET-based sensors. (b) The increased sensitivity in the 'Off' mode of a TFET-based sensor due to gate-tuning.

The dynamic range widening has also been demonstrated by Kalra *et al.* [8] through a tuned or reconfigured gate biasing i.e. the gate bias has been changed to achieve a wider dynamic range. This work also employs the same gate-tuning to obtain a wider dynamic range. However, the difference between these two works lies in the architecture of the sensor device; the work of Kalra *et al.* [8] involves a charge-plasma based device, whereas, the present work deals with a very simple p-i-n tunnel FET based sensor. The increased sensitivities in the 'off' mode due to gate-tuning are observed in Fig. 4 (b).

Fig. 5 provides a graphical presentation of the measurable pH-range against the average sensitivity of choice. Indeed, this graphical view depicts a characteristic feature obtained from a TFET based ISFET sensor that both wider pH range and higher sensitivity can be achieved by applying proper gate tuning and thus offering more flexibility in

terms of the choice of pH-measurement and sensitivity. However, if the chosen sensitivity is significantly higher this advantage of obtaining wider measurable pH range has been lost. It is noteworthy that MOSFET-based ISFETs have no such advantage of tuned dynamic range.

Table 1 summarizes the performance of the device and its comparison with the best ISFET sensors in the literature. Devices designed by Rignate et al. [1] and Cordera et al. [23], like most other ISFETs, are rather bulky, 10 µm × 20 µm in size, and have sensitivity indices (SI) under 0.6 dec/pH. Designs of more recent vintage, such as Zhang et al. [2] and Bellando et al. [17], managed to improve the SI to 1.2 dec/pH, yet have not been able to scale down channel dimensions, which remain 15 µm × 20 µm. The device developed in this work, a TFET-based ISFET, achieves the sensitivity index of 1.24–1.63 dec/pH, which is a record in the sensitivity-to-scalability trade-off, in addition to 1.24–1.63 dec/pH. It does this at a footprint of 1µm × 0.02 µm, which is record low for this class of devices. It is thus the most sensitive device out of all designs compared, while the dimensions are still the smallest. These results show how favorable TFET-based ISFETs are for next generation wearable sweat sensors. Their proposed architecture has high sensitivity, wide dynamic range, and strong scalability, allowing real time and accurate tracking of cellular, fluidic, and physiological pH changes for low sample volumes.

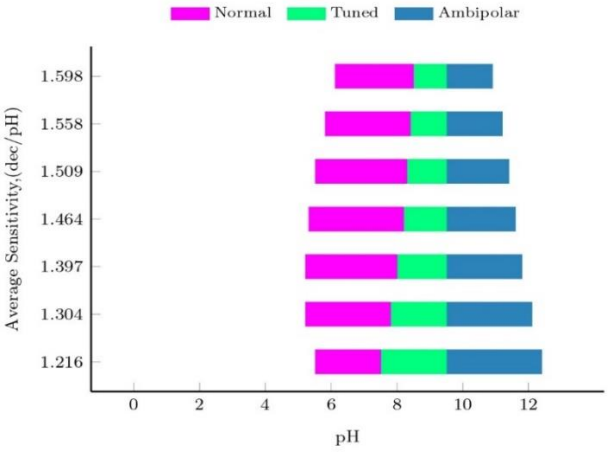

Fig. 5. Average sensitivity vs. measurable pH range of the gate-tuned TFET-based ISFET sensor.

Table 1. State-of-the-Art ISFET Sensors

SoA	S_I (dec/pH)	W× L (µm × µm)
Rignate *et al.* [1]	0.4	10×20
Cordera et al. [19]	0.59	10 ×20
Zhang et al. [2]	0.78	15×20

Bellando et al. [14]	1.2	15×20
This work	**1.24-1.63**	**1×0.02**

4 Conclusion

This study shows that a tunnel field-effect transistor (TFET) can serve as a strong alternative to conventional MOSFETs when used as the sensing element in an ionsensitive field-effect transistor (ISFET). Simulation results in Cadence confirm that when biased in the subthreshold region, the TFET-based ISFET responds with higher current sensitivity to changes in solution pH, making it more effective for detecting small variations. The natural ambipolar behavior of TFETs also enables tuning for a wider dynamic range, which broadens the scope of measurable pH values. In addition, the ability of TFETs to operate with smaller channel lengths without loss of performance provides improved scalability, reducing the required sample volume for accurate measurement. Taken together, these advantages position TFET-based ISFETs as a practical and efficient approach for sweat sensors and other biomedical applications that require precise, real-time monitoring of pH in cells, body fluids, and physiological systems.

Acknowledgments. The authors gratefully acknowledge the access and support provided by United International University for its licensed Cadence Tool Suite.

Disclosure of Interests. The authors have no competing interests.

References

1. Rigante, S. et al. Sensing with advanced computing technology: Fin field-effect transistors with high-k gate stack on bulk silicon. ACS nano, 9(5), 4872–4881 (2015).
2. Zhang, J. et al. Sweat biomarker sensor incorporating picowatt, three-dimensional extended metal gate ion sensitive field effect transistors. ACS sensors, 4(8), 2039–2047 (2019).
3. Bariya, M., Nyein, H. Y. Y. & Javey, A. Wearable sweat sensors. Nature Electronics, 1(3), 160–171 (2018).
4. Haque, A., Rahman, A. & Chowdhury, I. B. On the use of appropriate boundary conditions to calculate the normalized wave functions in the inversion layers of mosfets with ultra-thin gate oxides. Solid-State Electronics, 44(10), 1833–1836 (2000).
5. Chowdhury, M. I. B. Ion-sensitive vertical tunnel field-effect transistor for highly sensitive, low power, low ph-resolution ph sensing. IEEE Sensors Letters, 8(1), 1–4 (2024).
6. Amina, M., Biswas, P., Ullah, A. & Chowdhury, M. I. B. Analysis of common-mode rejection ratio of a CMOS differential amplifier considering all the non-idealities. In 2nd International Conference on Electrical Information and Communication Technologies (pp. 234–238) (2015).

7. Chakraborty, P. J., Islam, M. M., Ahamed, R. & Chowdhury, M. I. B. Sub-20nm gaas-based cylindrical gate-all-around fets for improved performance. In 2021 2nd International Conference on Robotics, Electrical and Signal Processing Techniques, pp. 473–477, IEEE (2021).
8. Kalra, S., Kumar, M. J. & Dhawan, A. Reconfigurable fet biosensor for a wide detection range and electrostatically tunable sensing response. IEEE Sensors Journal, 20(5), 2261-2269 (2019).
9. Emon, M. Z. A. et al. Switching power of cnfet based 6-transistor 1-bit fast adder implemented using cadence. Advances in Mathematics: Scientific Journal, 9(6), 3581–3592 (2020).
10. Chowdhury, M. I. B. et al. Silvaco TCAD based analysis of cylindrical gate-all-around FET having indium arsenide as channel and aluminium oxide as gate dielectrics. J. Nanotechnol. Appl. Eng., 1(1), 1–12 (2016).
11. Islam, M. J., Hasan, M. M., Farwah, S. U. & Chowdhury, M. I. B. A novel cylindrical gate all around MOSFET using InAs as channel and HfO2 as gate oxide. ISTP J Res Electric Electron Eng (ISTP-JREEE), special issue on ISTP (IOCRSEM-2014), 59–62 (2014).
12. Islam, M. J., Sami, R., Islam, M. S. & Chowdhury, M. I. B. Study of characteristics curves of top-gated graphene FET using Silvaco TCAD. J. Electron. Des. Eng., 3(3), 1–9 (2017).
13. Quader, S., Siddik, A. B., Hossain, N. M. & Chowdhury, M. I. B. Germanium silicon based hetero junction cylindrical gate all around field effect transistor for improved performance. International Journal of Engineering Technology, Management and Applied Science, 5(9), 1-6 (2017).
14. Bellando, F. et al. Subthermionic negative capacitance ion sensitive field effect transistor. Applied Physics Letters, 116(17), 173503 (2020).
15. Ionescu, A. M. & Riel, H. Tunnel field-effect transistors as energy efficient electronic switches. Nature, 479(7373), 329–337 (2011).
16. Singh, A., Narang, R., Saxena, M. & Gupta, M. Ambipolar behaviour of tunnel field effect transistor (tfet) as an advantage for biosensing applications. In Physics of Semiconductor Devices. Springer, 171–174 (2014).
17. Lee, R. et al. Investigation of feasibility of tunneling field effect transistor (tfet) as highly sensitive and multi-sensing biosensors. Journal of Semiconductor Technology and Science, 17(1), 141–146 (2017).
18. Rakhi, N. et al. Assessment of ambipolar behavior of a tunnel fet and influence of structural modifications. Journal of Semiconductor Technology and Science, 12(4), 482–491 (2012).
19. Garcia-Cordero, E. et al. Three-dimensional integrated ultra-low- volume passive microfluidics with ion-sensitive field-effect transistors for multiparameter wearable sweat analyzers. ACS nano, 12(12), 646–656 (2018).
20. Gao, X. P., Zheng, G. & Lieber, C. M. Subthreshold regime has the optimal sensitivity for nanowire fet biosensors. Nano letters, 10(2), 547–552 (2010).
21. Chowdhury, M. I. B. and Hassan, M. M. S. Analytical modeling of base transit time considering recombination in the non-uniformly doped base. In 2011 International Symposium on Humanities, Science and Engineering Research, pp. 117–122, IEEE (2011).
22. Islam, S. M. M., Chowdhury, M. I. B., Arafat, Y. & Khan, M. Z. R. Base transit time of a heterojunction bipolar transistor (hbt) with gaussian doped base under high-level of injection. In 2012 International Conference on Devices, Circuits and Systems, pp. 114–118, IEEE (2012).
23. Islam, M.J., Hasan, M.M., Sami, R. and Chowdhury, M.I.B. Modeling of graphene/sio2/si (n) based metal-insulator-semiconductor solar cells. In 2016 4th International Conference

on the Development in the in Renewable Energy Technology (ICDRET), pp. 1-4, IEEE (2016).
24. Biswas, P., Hasan, A.S., Rahim, A.B., Ullah, A. and Chowdhury, I.B., 2015, December. Analytical approach of JV characteristics of CdTe based thin film solar cells including voltage and space dependent electric field in the absorber layer. In 2015 2nd International Conference on Electrical Information and Communication Technologies (EICT), pp. 446-450, IEEE (2015).
25. Siddik, A. B., Hossain, N. M., Quader, S. & Chowdhury, M. I. B. Silicon on metal technology merged with cylindrical gate all around fet for enhanced performance. In 2017 3rd International Conference on Electrical Information and Communication Technology, pp. 1–4, IEEE (2017).
26. Hossain, N. M., Quader, S., Siddik, A. B. & Chowdhury, M. I. B. Tcad based performance analysis of junctionless cylindrical double gate all around fet up to 5nm technology node. In 2017 20th International Conference of Computer and Information Technology, pp. 1–4, IEEE (2017).
27. Quader, S., Siddik, A.B., Hossain, N. M. & Chowdhury, M. I. B. Channel engineered cylindrical double gate all around FET for low power VLSI applications. In 2018 International Conference on Computer, Communication, Chemical, Material and Electronic Engineering, pp. 1-4, IEEE (2018).
28. Rahamoni, M. T., Kabir, S., Parvez, M. H., Islam, S. & Chowdhury, M. I. B. Towards the portability of a capacitive-sensor based non-invasive glucometer: A simulation approach. In 2020 IEEE International Women in Engineering (WIE) Conference on Electrical and Computer Engineering, pp. 94–97, IEEE (2020).
29. Shovon, S. K. F. A., Sohan, R. R., Dhurba, T. D., Ghosh, S. K., Islam, M. J. & Chowdhury, M. I. B. Proteus-Matlab Based Implementation and Filter Performance Analysis of an Analog Front-End Circuit for ECG Signal Processing. Journal of Advancement in Electronics Signal Processing, 2(2), 1-12 (2025).
30. Islam, A. & Chowdhury, M. I. B. A simulink-based generalized model of PV cell/array. In 2014 3rd International Conference on the Developments in Renewable Energy Technology, pp. 1-5, IEEE (2014).
31. Islam, A. & Chowdhury, M. I. B. Simulation of two-diode model based PV solar cell/array: A SIMULINK approach. ISTP Journal of Research in Electrical and Electronics Engineering (ISTP-JREEE), Special Issue on 1st International Conference on Research in Science, Engineering & Management, pp. 67-72, (2014).
32. Emon, M. Z. A., Salim, K. M. & Chowdhury, M. I. B. Design and analysis of a high-gain, low-noise, and low-power analog front end for electrocardiogram acquisition in 45 nm technology using gm/id method. Electronics, 13(11), 2190 (2024).
33. Emon, M. Z. A. & Chowdhury, M. I. B. Low threshold voltage mosfet- a potential candidate for biomedical ic design. In 2024 International Conference on Advances in Computing, Communication, Electrical, and Smart Systems, pp. 1–6, IEEE (2024).
34. Zubair, M. Z. A., Salim, K. M. & Chowdhury, M. I. B. A study on source degenerated telescopic OpAmp for biomedical applications. Lecture Notes in Electrical Engineering, 339–353, Springer (2025).
35. Martinoia, S. & Massobrio, G. A behavioral macromodel of the isfet in spice. Sensors and Actuators B: Chemical, 62(3), 182–189 (2000).
36. Dak, P., Seo, W., Jung, B., & Alam, M. A. A physics-based (verilog- a) compact model for dc, quasi-static transient, small-signal, and noise analysis of mosfet-based ph sensors. IEEE Transactions on Electron Devices, 64(3), 1285–1293 (2017).

37. Lu, H., Ytterdal, T. & Seabaugh, A. Universal TFET Model. https://nanohub.org/publications/31/1 (2015).
38. F´erard, G. Quantities and units for electrophoresis in the clinical laboratory (iupac recommendations 1994). Pure and applied chemistry, 66(4), 891–896 (1994).